758

INSTITUT DE PHYSIQUE DE L'UNIVERSITÉ DE NEUCHÂTEL

# Thermal Disorder of Silver Bromide Studied by 100 keV Proton Channeling

RÉSUMÉ DE LA THÈSE

présentée
à la Faculté des Sciences de l'Université de Neuchâtel
pour l'obtention du grade de docteur ès sciences

par

MICHEL ROULET
physicien diplômé

1976

phys. stat. sol. (a) 35, 97 (1976)

Subject classification: 10.2; 11; 22.5.1

*Institut de Physique de l'Université, Neuchâtel*

# Thermal Disorder of Silver Bromide Studied by 100 keV Proton Channeling[1])

By

M. ROULET, H. HUBER, and C. JACCARD

Channeling is measured in single crystals of AgBr between 90 and 595 K. The experimental dechanneling is separated in one part due to thermal vibrations of atomic rows and in another part due to silver interstitials with a cross section increasing from 4.4 to 5.0 $\times$ $\times 10^{-17}$ cm$^2$ between 445 and 595 K. A formation energy of (0.65 $\pm$ 0.10) eV is determined and a molar concentration of Frenkel defects varying from 0.003 to 0,03 between 445 and 595 K. The concentration extrapolated to 695 K amounts to 0.06 $\pm$ 0.02 (melting point: 697 K). Furthermore Meyer's theory of plural and multiple scattering is checked at low energy with a silver thin film evaporated on a AgBr crystal.

La canalisation est mesurée dans des monocristaux d'AgBr entre 90 et 595 K. La décanalisation expérimentale est séparée en une partie due aux vibrations thermiques des chaînes atomiques et en une autre partie due à des interstitiels d'argent dont la section efficace augmente de 4,4 à 5,0 $\times$ $10^{-17}$ cm$^2$ entre 445 et 595 K. Nous déterminons une énergie de formation des défauts de Frenkel variant de 0,003 à 0,03 entre 445 et 595 K. La concentration, extrapolée à 695 K se monte à 0,06 $\pm$ 0,02 (point de fusion: 697 K). De plus, nous vérifions la théorie de Meyer de la diffusion plurale et multiple à basse énergie avec un film mince d'argent évaporé sur un cristal de AgBr.

## 1. Introduction

Discovered in 1962 by Oen and Robinson [1], the channeling effect has been widely studied in various crystals during the last decade, and it has also been used as a tool in order to solve some problems of solid state physics. This paper presents such a case, in which channeling gives valuable information on lattice disorder. The effect is conceptually very simple. Most of the particles of a beam, entering a lattice along a main crystallographic direction, are confined within the channels formed by the atomic chains by small angle scattering and their probability for a nuclear encounter is very small. In the case of Rutherford backscattering, the yield shows a sharp minimum when the crystal is aligned with respect to the beam. The depth of the minimum is related to the lattice perfection. Moreover, energy analysis of the backscattered particles yields a depth scale for the nuclear encounters, if the stopping power of the material is known. A detailed account of the relevant parameters, such as the minimum yield, the critical angle, the dechanneling rate and also of many applications can be found in a recent review by Gemmell [2].

Silver bromide has been chosen to apply the channeling method for the following reasons. It is possible to obtain this substance as good quality monocrystals with a simple structure, the atomic number is high (giving a large scattering cross section), and the thermal disorder reaches at high temperature

[1]) This work has been performed by M. Roulet as partial fulfilment of a PhD thesis.

a level which produces a significant effect. On the other hand, the question of lattice defects at high temperature is not yet settled, although AgBr is one of the best studied crystals since 1936. Measurements of electrical conductivity [3 to 7] and of specific heat [8, 9] have revealed the existence of Frenkel disorder of cationic type, supported by X-ray measurements of the thermal expansion [10, 11]. However, the agreement between the different methods is only partial, and it justifies a new approach by use of the channeling effect.

In this paper, we present first the experimental set-up and then the results for the critical angle, the temperature dependence of the minimum yield, and the dechanneling cross section of silver obtained from a thin metallic surface layer. These parameters are discussed in Section 4, together with the concentration of silver interstitials as a function of temperature, which is then compared with the results obtained by other methods. The effect of a thin metallic layer is discussed in terms of Meyer's theory of plural and multiple scattering of low-energy heavy particles in solids [12].

## 2. Experimental

Single crystals of silver bromide grown by Verneuil's method have been kindly supplied by Dr. P. Junod (Ciba-Geigy Laboratories). The total concentration of impurities is less than 10 ppm. Samples of 1 $cm^3$ are cut with a face perpendicular within less than 2° to the ⟨100⟩ axis. Since the crystals cannot be cleaved, a clean surface is prepared by chemical etching (5 min in a solution of KCN 1 N). The samples are mounted on a goniometer with two degrees of freedom for rotation and two for translation. The crystal can be oriented with a precision of 0.05°. The temperature can be varied between 90 and 700 K. The crystal is bombarded with a 100 keV proton beam (divergence $<0.05°$, diameter 0.3 mm, current 0.1 to 10 nA). The scattering chamber is evacuated up to $2 \times 10^{-6}$ Torr with a diffusion pump through a liquid nitrogen trap. To prevent surface contamination especially at low temperature the crystal is surrounded by another trap at LNT.

Backscattered protons are detected at 150° with a 50 $mm^2$ surface barrier detector silicon (ORTEC PREMIUM SERIES), cooled at $(-80 \pm 5)$ °C in order to obtain an energy resolution of 4 to 6 keV (FWHM) corresponding to a depth resolution of 60 to 90 Å for AgBr. The detector is connected to high resolution standard electronics followed by a 256 multichannel analyser and a single channel analyser. The spectra are recorded analogically with a strip-chart recorder or digitally with a punched paper type, which can be fed to a computer. The multichannel energy calibration is achieved by scattering of 50 and 100 keV protons on heavy rare gases.

In the 100 keV energy range, the stopping power of protons is maximum (at 100 keV: 22.1 eV/Å for Ag and 15.7 eV/Å for Br [13]) and it is almost the same for channeled and for random directions, since only valence electrons contribute to the stopping power in the region where it is maximum [14]. This has been checked for example in silicon [27]; the ⟨111⟩ channeled stopping power is smaller by less than 5% than the random one, the deviation being due to the inhomogeneity of the valence electron density. This slight difference can be neglected in first approximation in our case since the accuracy of the stopping power amounts to 5 to 10% and we have anyway other sources of error.

The proton dose is measured by integrating with an electrometer a part of the beam intercepted by a nickel grid (cell size $100 \times 100\,\mu m^2$). A second grid (cell size $10 \times 10\,\mu m^2$), 2 cm in front of the crystal, is used to emit secondary electrons, which compensate for the proton charge on the insulating sample, without destroying the collimation. We checked the absence of sample contamination by sputtered nickel atoms by backscattering on light targets such as beryllium or ice. We can alternatively compensate with secondary electrons produced by ion bombardment of a screen suitably positioned near the crystal.

## 3. Results

### *3.1 Critical angle and minimum yield*

At room temperature the relative minimum yield is $\chi = (20.0 \pm 0.5) \times 10^{-2}$ for alignment in the ⟨100⟩ direction. The critical angle is taken as the half-width at half-depth: $\psi_{1/2} = (2.0 \pm 0.1)^0 = (3.5 \pm 0.2) \times 10^{-2}$ rad at RT and $(2.5 \pm \pm 0.1)^0$ at 90 K. The choice of the tilting plane (0, 13, 3) is achieved by means of a stereographic chart, in which the intersection of planar channeling directions defines the channel axis. A typical dose of $10^{-2}$ $H^+$/channel, obtained by shifting the sample with respect to the beam, avoids any significant radiation damage.

The kinematic energy loss of protons being 4.6% on bromine and 3.4% on silver nuclei, the energy of the detected particles in our experiment extends below 96 keV. Energy distribution spectra are shown in Fig. 1 above and below room temperature with depth resolution of 90 and 60 Å, respectively ($\Delta E = 6$ and 4 keV FWHM, respectively). The depth scale given in the upper part of the diagram is derived from the stopping power. The upper dashed line pertains to a beam incident in a random direction, whereas the lower full lines corre-

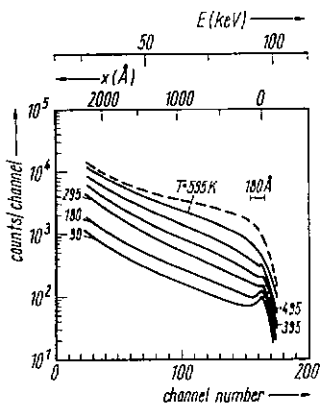


Fig. 1

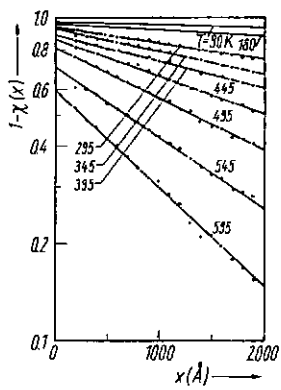


Fig. 2

Fig. 1. Channeling between 90 and 595 K for 100 keV $H^+$ along the ⟨100⟩ direction in AgBr. Full line: channeled spectrum; dashed line: random spectrum. Depth resolution: 60 to 90 Å. Energy calibration: 0.500 keV/channel. Scattering angle: 150°

Fig. 2. Channeled normalized component versus depth between 90 and 595 K for 100 keV $H^+$ along the ⟨100⟩ direction in AgBr

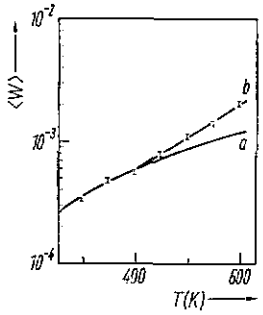


Fig. 3. Dechanneling probability per atomic layer along the ⟨100⟩ direction for 100 keV $H^+$ in AgBr. (a) theoretical curve valid for a perfect vibrating crystal; (b) experimental curve

spond to a well aligned beam in the ⟨100⟩ direction. The ratio of both spectra as a function of the depth gives the minimum yield $\chi$. All channeled spectra display a small peak near the surface, produced by the "heads" of the atomic rows. Using Rutherford cross section, its area is found to correspond to 2 to 3 disordered atomic layers, which is quite normal for good crystals and shows that the chemical surface treatment is adequate. The channeled spectra are independent of thermal cycles; this suggests that the process governing the lattice disorder is reversible.

The minimum yield grows with depth $x$ and temperature from a value of $3 \times 10^{-2}$ (extrapolated at the surface at 90 K) and according to the law

$$1 - \chi(x, T) = [1 - \chi(0, T)] \exp\left\{-\langle W(T)\rangle_e \frac{x}{d}\right\} \tag{1}$$

represented in Fig. 2, $d$ being the separation between the layers.

The experimental values of the dechanneling probability per atomic layer $\langle W(T)\rangle_e$ are plotted versus temperature in curve b of Fig. 3.

### *3.2 Dechanneling cross section of silver*

For a crystal covered with a thin amorphous or polycrystalline film, the increase of the surface minimum yield can be used to obtain the dechanneling cross section of the atoms of the film (see Section 4.2). Fig. 4 shows the minimum yield and the channeled spectrum for a crystal at 90 K covered with an evaporated silver film of (140 ± 20) Å. The film thickness is measured by counting the area of the silver peak defined either by the dashed line of Fig. 4 or by the peak of silver evaporated at the same time on a light material such as beryllium. This peak is well defined since the kinematic elastic loss is ten times smaller

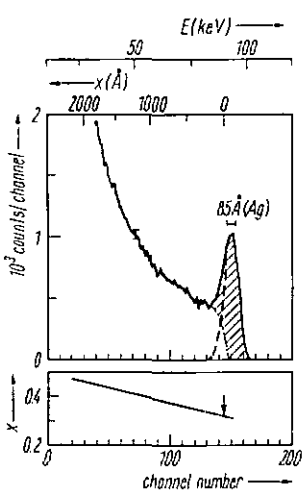


Fig. 4. Channeled spectrum and minimum yield at 90 K for 100 keV $H^+$ along the ⟨100⟩ direction in AgBr covered with a silver layer of (140 ± 20) Å. Dashed line: silver spectrum; dot-dashed line: AgBr spectrum. The position of the underlying crystal is marked. Depth resolution (Ag): 43 Å. Energy calibration: 0.550 keV/channel. Scattering angle: 150°

on silver than on beryllium. We get a thickness of (140 ± 20) Å in this case and (130 ± 20) Å with Fig. 4, where the dashed line is the mirror image of the high energy flank as discussed in [15]. The thin evaporated film increases the minimum yield from 0.03 to 0.32 and the dechanneling rate $d\chi/dx$ by a factor of two to four. Setting the window of the single channel analyser on the silver film, we have checked the lack of channeling in it. Therefore it appears as amorphous or polycrystalline with randomly oriented crystallites.

## 4. Discussion

### *4.1 Critical angle and surface minimum yield*

Lindhard [16] defines the maximum angle $\Psi_L$ for which his continuum potential is valid to describe an atomic row:

$$\Psi_L = \Psi_1 = \sqrt{\frac{2Z_1 Z_2 e^2}{Ed}} \quad \text{for } \Psi_1 \lessapprox \frac{a}{d} \text{ (high energy range)}, \tag{2}$$

$$\Psi_L = \Psi_2 = \sqrt{\sqrt{\frac{3}{2}} \frac{a}{d} \Psi_1} \quad \text{for } \Psi_1 > \frac{a}{d} \text{ (low energy range)}, \tag{3}$$

where $E$ is the energy of the incident particle, $d$ the interatomic distance along the row, $Z_1$ the atomic number of the incident particle, $Z_2$ the atomic number of the atoms of the crystal, and $a$ the Thomas-Fermi radius. He proposes for the critical angle: $\Psi_c = C\Psi_L$ with $C \approx 2$. $\Psi_L$ has an order of magnitude of $10^{-2}$ to 10°. Barrett's Monte Carlo calculations [17] give $\Psi_c = \Psi_{1/2}$ as a function of the temperature:

$$\Psi_{1/2} = kR\left(\frac{mu_1}{a}\right)\Psi_L, \tag{4}$$

$k$ and $m$ being fitted parameters. For axial channeling $k = 0.72$, $m = 1.0$ in the low energy range and $k = 0.80$, $m = 1.2$ in the high energy range. $R$ is a tabulated function and $u_1$ is the r.m.s. thermal displacement perpendicular to the row, obtained from Debye's theory:

$$u_1^2 = \frac{3h^2}{Mk\theta_D} \frac{T}{\theta_D} \{\Phi(x) + 0.25x\} \tag{5}$$

with $x = \theta_D/T$. According to Lonsdale [18], $M$ is to be taken as the average mass of the constituents.

For silver bromide, $\theta_D = 144$ K and we have typically $u_1^2 = 4.4 \times 10^{-18}$ cm² at 600 K. We use for $Z_2$ the average atomic number since silver and bromine are relatively close in the periodic table of the elements.

Equation (4) has been checked by many authors [17, 19] for metals, semiconductors, and insulators. It always gives $\Psi_{1/2} < \Psi_L$, showing the great importance of thermal vibrations which are not included in Lindhard's estimation. For 100 keV protons along ⟨100⟩ in AgBr, $\Psi_L$ is equal to $\Psi_2 = 3.5°$ ($\Psi_1 = 3.7° > a/d = 0.136$ Å/2.89 Å = 2.7°; we are just below the limit of the high energy range). Using equation (4) we get at 295 K (with $k = 0.72$ and $m = 1.0$) $\Psi_{1/2} = 0.56\Psi_2 = 2.0°$ in good agreement with the experimental value of (2.0 ± 0.1)°. At 90 K the experimental value is (2.5 ± 0.1)° compared to the theoretical one of 2.5°. At high temperature the minimum yield is so

large that it is no longer possible to identify the experimental $\Psi_{1/2}$ value with the critical angle $\Psi_c$; it is more convenient to use equation (4).

The surface minimum yield has been estimated by Lindhard [16], but his equation always gives values smaller than the experimental results. Barrett [17] has improved the theoretical approach by Monte Carlo calculations. He proposes an equation valid near the surface which stresses thermal vibrations and which is usually compared with the minimum yield extrapolated to the surface or close to it:

$$\chi = \frac{C2\pi u_1^2 + C'\pi a^2}{A} \tag{6}$$

with $C = 3.0 \pm 0.2$, $C' = 0.2 \pm 0.1$, and $A$ surface of the channel. The comparison of the surface minimum yield (Fig. 2) with equation (6) shows that experimental values are 1 to 2 times greater up to 495 K and about 3 times greater for higher temperature. This difference may be explained by a slight surface disorder not visible in the energy spectrum and by the fact that $C$ and $C'$ have been determined for energies and projectile–target combinations different from ours. (Barrett finds actually an increase of the minimum yield with decreasing energy, confirmed by experiments on germanium [30].)

### *4.2 Dechanneling cross section of silver*

According to Lindhard [16] an increase $\Delta\chi$ of the minimum yield occurs when the surface is contaminated:

$$\Delta\chi = \frac{\sum_s n_s f_s \sigma_d^s}{A}. \tag{7}$$

$s$ labels the type of atom, $n_s$ is the number of equivalent amorphous monolayers, $f_s$ the overlapping factor ($f_s = N_s^{2/3}/N^{2/3}$, $N_s$ and $N$ being the atomic density in the layer and in the crystal, respectively), $\sigma_d^s$ the dechanneling cross section and $A$ the channel area. For silver on AgBr we have $f = 1.25$, $A_{\langle 100\rangle} = 8.35 \times \times 10^{-16}$ cm$^2$. Table 1 presents results for the silver evaporation of (140 ± 20) Å at 90 K (Fig. 4) and at 295 K and the evaluation of the scattering cross section according to (7). The last line shows values calculated by means of a theory

Table 1

Effect of a silver film on the minimum yield in axial channeling of 100 keV protons in AgBr and derived silver dechanneling cross-section

| $T$ (K) | 90 | | 295 | |
|---|---|---|---|---|
| | AgBr | AgBr(Ag) | AgBr | AgBr(Ag) |
| $d\chi/dx$ ($10^{-4}$ Å$^{-1}$) | 0.2 | 0.7 | 1.0 | 2.0 |
| $\chi \times 10^2$ | 3.0 ± 0.5 | 32.0 ± 0.5 | 6.5 ± 0.5 | 42.0 ± 1.0 |
| $\Delta\chi \times 10^2$ | 29.0 ± 1.0 | | 35.5 ± 1.5 | |
| $\Delta\chi/\Delta x$ ($10^{-3}$/Ag monolayer) | 5.4 ± 1.0 | | 6.6 ± 1.3 | |
| $\sigma_d$ (Ag) ($10^{-18}$ cm$^2$) | 5.6 ± 1.0 | | 6.9 ± 1.3 | |
| $\sigma_d$ (Ag) theoretical ($10^{-18}$ cm$^2$) | 3.8 ± 0.4 | | 5.3 ± 0.5 | |

developed by Lindhard et al. [20], using a reduced energy

$$\varepsilon = \frac{1}{2}\frac{m_1 m_2}{(m_1 + m_2)} v^2 \left(\frac{Z_1 Z_2 e^2}{a}\right)^{-1}$$

and a reduced angle

$$\eta = \varepsilon \sin\frac{\theta}{2},$$

where $\theta$ is the scattering angle in the centre of mass system. The cross section is given by

$$\sigma_d = \pi a^2 \int_{\eta_c}^{\varepsilon} \frac{f(\eta)}{\eta^2}\,d\eta\,,$$

where $f(\eta) \approx (2\eta + 1.58 + 0.17\eta^{-1/2})^{-1}$ describes the screening of the potential [12] and $\eta_c$ corresponds to the critical angle.

Table 1 shows that the amorphous or polycrystalline silver layer on the AgBr single crystal increases the minimum yield and the rate of dechanneling. The dechanneling cross section increases with temperature. Experimental values of $\sigma_d$ are a little larger than theoretical ones. At 295 K they are consistent, but at 90 K the errors do not overlap exactly. This can be attributed to the uncertainty attached to the critical angle and to the oversimplification of expression (7).

For silver atoms in the channels inside the crystal, the dechanneling cross section has to be corrected because of three effects.

(i) The inelastic losses make the energy to range between 100 and 68 keV in a depth of 2000 Å. This produces an average increase of $\sigma_d$ by 25% with respect to 100 keV.

(ii) The critical angle $\Psi_c$ varies with temperature and it introduces a dependence expressed by $\sigma_d \approx 6.6 \times 10^{-18}\,[1 + 6 \times 10^{-3}\,(T - 295\ \mathrm{K})]\ \mathrm{cm}^2$ above 295 K and a decrease to $4.8 \times 10^{-18}$ cm$^2$ down to 90 K.

(iii) Inside the crystal, the proton trajectories make with the channel axis an angle $\Phi$ which is distributed almost evenly between zero and $\Psi_c$ according to the function $2\Phi/\Psi_c^2$. The protons remain channeled provided their scattering angle is smaller than an angle $\vartheta_m$ related by elementary geometry with $\Psi_c$ and $\Phi$ by the expression $\Psi_c^2 \approx \Phi^2 + \vartheta_m^2 + 2\Phi\vartheta_m \cos\varphi$. This defines a maximum value for the reduced parameter: $\eta_m \simeq \frac{1}{2}\varepsilon\vartheta_m$. The average cross section is obtained by a triple integration:

$$\bar{\sigma}_d \approx \pi a^2 \int_0^{\Psi_c} \frac{2\Phi\,d\Phi}{\Psi_c^2} \int_0^{\pi} \frac{d\varphi}{\pi} \int_{\eta_m}^{\infty} \frac{f(\eta)}{\eta^2}\,d\eta\,.$$

It is interesting to compare this value with that corresponding to a trajectory parallel to the channel ($\Phi = 0$), in the high temperature range:

$$\bar{\sigma}_d \approx 6\ \sigma_d(\Phi = 0)\,.$$

### *4.3 Concentration of silver interstitials*

The strong temperature dependence of the channeled spectra shown in Fig. 1 cannot be explained only by thermal vibrations of atomic rows. It requires another dechanneling mechanism: the silver interstitials introduced earlier to explain electrical conductivity and specific heat measurements.

The logarithmic plot of $1 - \chi(x)$ versus the depth $x$ (Fig. 2) shows that the exponential Ansatz of equation (1) is convenient for $0 \leqq x \leqq 2000$ Å. Its main parameter is $\langle W \rangle_e$, the experimental dechanneling probability per atomic layer, valid for the bulk of the crystal, to which two processes contribute: the thermal vibrations of the rows and the scattering by the silver interstitials. The dechanneling probability per monolayer $\langle W \rangle_T$ by the former process can be taken from Kumakhov's statistical theory [22]. For the latter process, it is given by $N_0 c \bar{\sigma}_d d$, where $N_0 = 2.08 \times 10^{22}$ mol/cm³ is the molar density of AgBr, $c$ the molar concentration of silver interstitials, $\bar{\sigma}_d$ their dechanneling cross section, and $d = 2.89$ Å is the distance between layers.

We do not introduce any sharp flux peaking effect for the dechanneling probability by the silver interstitials for the following reason. Computer simulations of particle flux [28, 29] have shown that it requires a certain depth to develop and that it is characterized by strong depth oscillations (larger than our depth resolution) which do not show up in the high temperature range where $\langle W \rangle_e$ is constant. Moreover, thermal vibrations are known to damp flux peaking effects.

The molar concentration becomes then

$$c = \frac{\langle W \rangle_e - \langle W \rangle_T}{N_0 \bar{\sigma}_d d}. \tag{8}$$

In Fig. 3 we have plotted $\langle W \rangle_T$ (curve a) and $\langle W \rangle_e$ (curve b). Up to 400 K the agreement between the theoretical values valid for a perfect vibrating crystal and the experimental ones is good, but for $T > 400$ K we have a difference increasing with temperature. It is significant, since at about 600 K the experimental value is twice the experimental one. Admitting that the agreement between the two curves up to 400 K allows to extrapolate curve *a* for the dechanneling probability due to thermal vibrations, we can relate the difference between *a* and *b* to the silver interstitial concentration given by equation (8).

Table 2 gives at high temperature the molar concentration of silver interstitials and the characteristic data used to determine it. The error given for $c$ contains only the error on $\langle W \rangle_e$. We have not included the systematic errors due to depth scale (the stopping power is known only with an accuracy of 5 to 10%) neither to $\sigma_d$ known within 10% according to Lindhard [21].

Table 2

Critical angle, dechanneling cross-section, dechanneling probability, and concentration of silver interstitials in AgBr

| $T$ (K) | $\Psi_c \times 10^2$*) | $\bar{\sigma}_d$ ($10^{-17}$ cm²) | $\langle W \rangle_e - \langle W \rangle_T$ ($10^{-4}$/layer) | $c(T) \times 10^2$ |
|---|---|---|---|---|
| 445 | 3.15 | 4.4 | 0.82 | $0.31 \pm 0.15$ |
| 495 | 3.06 | 4.6 | 2.4 | $0.87 \pm 0.20$ |
| 545 | 2.98 | 4.8 | 3.9 | $1.35 \pm 0.25$ |
| 595 | 2.90 | 5.0 | 8.6 | $2.85 \pm 0.35$ |

*) With equation (4).

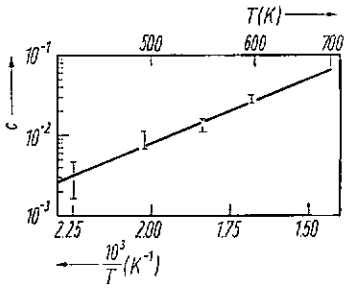


Fig. 5. Molar concentration of silver interstitials in AgBr

The logarithm of the concentration is plotted in Fig. 5 versus the reciprocal of the temperature. In spite of the narrow range of temperature, we see that the temperature dependence looks like a thermally activated process given by $c(T) = \text{const} \exp(-E_F/2kT)$, $E_F$ being the formation energy. The slope of the corresponding straight line gives $E_F = (0.65 \pm 0.10)$ eV. Extrapolating to 695 K (melting point $T_m = 697$ K) yields a concentration $c = 0.06 \pm 0.02$.

As to the distribution of interstitials, it is homogeneous in comparison with our depth resolution, since $\langle IV \rangle_c$ is depth independent (Fig. 2). Therefore the inhomogeneity, which appears near the crystal surface, mentioned by Kliewer [23] for AgCl and AgBr, cannot be studied by channeling.

Our results are explained by silver interstitials, also required for electrical conductivity, specific heat, and thermal expansion measurements. In Table 3

Table 3

Formation energy and molar concentration of Frenkel defects near the melting point according to various sources

| method | author | ref. | date | $E_F$ (eV) | $c$ (695 K) |
|---|---|---|---|---|---|
| electrical conductivity | Koch und Wagner | [3] | 1938 | 0.87 | 0.021 |
| electrical conductivity | Teltow | [4] | 1949 | 1.27 | 0.013 |
| electrical conductivity (DH) | Weber and Friauf | [5] | 1969 | 1.13 | — |
| specific heat excess | Christy and Lawson | [8] | 1951 | 1.28 | 0.037 |
| thermal expansion | Lawn | [11] | 1963 | 0.59 | — |
| electrical conductivity | Müller | [6] | 1965 | 1.06 | 0.025 |
| specific heat excess | Jost and Kubaschewski | [9] | 1968 | 1.41 | 0.024 |
| electrical conductivity (DH) | Aboagye and Friauf | [7] | 1975 | 1.13 | — |
| channeling | | | | $0.65 \pm 0.10$ | $0.06 \pm 0.02$*) |

DH: with Debye-Hückel interactions.
*) Extrapolated value.

we summarize data for formation energy and concentration of interstitials just below the melting point found by some authors with different methods.

The common feature of Table 3 is the high concentration of interstitials at high temperature. Discrepancies between one author and another appear

even for a given method. Electrical conductivity results take into account the vacancy mobility measured in divalent cation doped crystals. Some authors have tried to introduce long-range Debye-Hückel interactions valid for strong electrolytes. Because of the great disorder shown by Teltow in AgBr, Mott and Gurney [24] proposed to measure specific heat. This has been done by Christy and confirmed by Jost. They interpret the difference between the measured and the extrapolated specific heat (above 420 K) by the creation of Frenkel defects. However, Nölting [25] has compared specific heat measurements of AgBr with those of other crystals. In aluminium for example the Schottky disorder measured by thermal expansion is about half of the one determined by specific heat. This invalidates the mere linear extrapolation near the melting point, where anharmonic vibrations could contribute significantly to the specific heat.

The concentration at 695 K obtained by channeling is a little larger than the data from other methods; this might be due to the systematic errors mentioned above. As to the formation energy, our value is smaller than specific heat and electrical conductivity determinations. However, our value is quite similar to Lawn's result [11] determined from the anomalous thermal expansion.

As yet we have not taken into account the position and the interactions of silver interstitials. According to Hove's dumbbell model [26] a silver ion should not occupy a minimum energy position, when it is at the centre of a cube. The interstitialcy migration along ⟨111⟩ should displace with a very small energy expenditure a lattice silver ion creating this way a second interstitial. This process is explained by $Ag^+$ attraction by the (111) $Br^-$ plane and by the expulsion along ⟨111⟩ of a second silver ion. The equilibrium position of the pair corresponds to a dumbbell with its centre in a (111) silver plane and with its extremities close to the (111) bromine plane (the three $Br^-$ ions next to each dumbbell are relaxed) and 0.7 Å from the ⟨100⟩ channel centre, i.e. equivalent to a central position in the absence of sharp flux peaking. The dumbbell can be collinear or not. Weber and Friauf [5] use this dumbbell model in order to compare radioactive silver diffusion measurements with electrical conductivity measurements with the help of the Nernst-Einstein relation. These interstitialcy motion processes therefore increase the number of interstitial silver ions, decrease the mean formation energy of one interstitial and explain qualitatively the rather large values of the concentration and the formation energy obtained by channeling. The former is of course the absolute concentration of interstitials and not the dumbbell concentration. Aboagye and Friauf [7] measured recently again the ionic conductivity of AgBr and they conclude also large concentrations at high temperature. They show indeed that, even with Debye-Hückel interactions, the conductivity extrapolated at high temperature is less than the experimental one. This significant anomaly is interpreted by some additional Frenkel defects corresponding actually to a decrease of the formation energy quoted in Table 3, when the temperature increases. The enhancement of their concentration amounts to about a factor of 3 leading to a concentration of a few percent at the melting point.

The influence of the vacancies associated with the interstitials is difficult to establish. As a first approximation it can be neglected as well as the lattice deformation around an interstitial. However, any disturbance of the atomice row periodicity is a cause of dechanneling and the vacancies should play a minor role.

We have not taken into account additional thermal parameters such as enhanced vibrations of the rows near the interstitials or such as a modification of the transversal energy distribution of the channeled beam by interstitials. These effects could enhance the dechanneling and therefore lower our interstitial concentration. A slight flux peaking would have the same effect and, if temperature dependent, it would reduce the apparent formation energy.

#### *4.4 Dechanneling by a thin silver film*

The silver evaporation on AgBr mentioned in Section 4.2 modifies channeling: the minimum yield and the dechanneling increase. A theoretical estimation of the former can be made with Meyer's theory on plural and multiple scattering of low-energy heavy particles in solids [12]. Using three dimensionless parameters, he calculates the angular differential distribution of a beam of particles after penetration of a film with a given reduced thickness $\tau = \pi a^2 N t$ ($a$ being the Thomas-Fermi radius, $N$ the atomic density of the film and $t$ its thickness).

The angular distribution attained by the initially collimated beam after having passed through the film can be integrated on its wings from $\vartheta$ to $\pi$ and gives a function $P(\vartheta)$. The minimum yield is then related to $P$ and $\Psi_c$ by

$$\chi = P(\Psi_c) + \chi_s[1 - P(\Psi_c)] ,$$

$\chi_s$ being the minimum yield without the film.

We have evaporated a silver film on AgBr with a reduced thickness $\tau = 0.43 \pm 0.06$ corresponding to Meyer's multiple scattering. At 295 and 90 K, the theoretical values of $(45 \pm 9) \times 10^{-2}$ and $(34 \pm 7) \times 10^{-2}$ agree with the experimental values of $(42 \pm 1) \times 10^{-2}$ and $(32 \pm 0.5) \times 10^{-2}$, respectively. This demonstrates the validity of Meyer's treatment of multiple scattering at low energy.

## 5. Conclusion

Silver bromide is adequate for channeling experiments. Large single crystals can be grown and a clean undisturbed surface can be easily prepared by chemical etching in a potassium-cyanide solution.

A channeling study by the Rutherford backscattering technique of Frenkel defects in AgBr at high temperature makes a connexion with thermodynamics. Our results are similar to the ones obtained by electrical conductivity and specific heat experiments and especially by thermal expansion. However, the defect concentration of $0.06 \pm 0.02$ near the melting point is little larger and the formation energy of $(0.65 \pm 0.10)$ eV is somewhat smaller except for the last method. The discrepancies can be understood qualitatively by Hove's dumbbell model for silver interstitials in AgBr or by the temperature dependence of the formation energy shown in the latest electrical conductivity measurements by Aboagye and Friauf.

The effect of a thin silver film evaporated on AgBr is evaluated and channeling parameters obtained by Rutherford backscattering confirm Meyer's theory of plural and multiple scattering of low-energy heavy particles.

#### *Acknowledgements*

We are indebted to Dr. P. Junod (Ciba-Geigy Laboratories) for valuable discussions and to the Swiss National Foundation for the support of this work.

## References

[1] O. OEN and M. T. ROBINSON, Le bombardement ionique, C.N.R.S., Paris 1962.
[2] D. S. GEMMELL, Rev. mod. Phys. **46**, 129 (1974).
[3] E. KOCH and C. WAGNER, Z. phys. Chem. **B38**, 295 (1938).
[4] J. TELTOW, Ann. Phys. (Germany) **5**, 63 (1949).
[5] M. D. WERER and R. J. FRIAUF, J. Phys. Chem. Solids **30**, 407 (1969).
[6] P. MÜLLER, phys. stat. sol. **12**, 775 (1965); **21**, 693 (1967).
[7] J. K. ABOAGYE and R. J. FRIAUF, Phys. Rev. B **11**, 1654 (1975).
[8] R. W. CHRISTY and A. W. LAWSON, J. chem. Phys. **19**, 517 (1951).
[9] W. JOST and P. KUBASCHEWSKI, Z. phys. Chem. (N. F.) **60**, 69 (1968).
[10] C. R. BERRY, Phys. Rev. **82**, 422 (1951).
[11] B. R. LAWN, Acta cryst. **16**, 1163 (1963).
[12] L. MEYER, phys. stat. sol. (b) **44**, 253 (1971).
[13] A. VALENZUALA and W. MECKRACH, Phys. Rev. B **6**, 95 (1972).
[14] W. BRANDT, in: Compte Rendu du Congrès sur la canalisation, I.N.S.T.N. Saclay, May 1974, C.E.A., Saclay 1975 (p. 9).
[15] M. ROULET, Thesis, Univ. Neuchâtel, 1974.
[16] J. LINDHARD, Kong. Danske Vid. Selsk., mat.-fys. Medd. **34**, No. 14 (1965).
[17] J. H. BARRETT, Phys. Rev. B **3**, 1527 (1971).
[18] K. LONSDALE, Acta cryst. **1**, 142 (1948).
[19] D. V. MORGAN, Channeling, John Wiley & Sons, New York 1973.
[20] J. LINDHARD, V. NIELSEN, and M. SCHARFF, Kong. Danske Vid. Selsk., mat.-fys. Medd. **38**, No. 10 (1968).
[21] J. LINDHARD, Proc. Roy. Soc. (London) **A311**, 11 (1969).
[22] M. A. KUMAKHOV, Phys. Letters A **33**, 133 (1970).
[23] K. L. KLIEWER, J. Phys. Chem. Solids **27**, 705 (1966).
[24] N. MOTT and R. GURNEY, Electronic Processes in Ionic Crystals, Clarendon Press, Oxford 1950.
[25] J. NÖLTING, Angew. Chem. (Internat. Ed.) **9**, 489 (1970).
[26] J. E. HOVE, Phys. Rev. **102**, 915 (1956).
[27] G. DELLA MEA, A. V. DRIGO, S. LO RUSSO, P. MAZZOLDI, and G. G. BENTINI, in: Atomic Collisions in Solids, Ed. S. DATZ, B. R. APPLETON, and C. D. MOAK, Plenum Press, New York 1975 (p. 75).
[28] D. V. MORGAN and D. VAN VLIET, in: Atomic Collisions in Solids, Vol. 4, Ed. S. ANDERSEN et al., Gordon and Breach, London 1972 (p. 151).
R. B. ALEXANDER and J. M. POATE, ibid. (p. 159).
J. U. ANDERSEN, E. LEGSGAARD, and L. C. FELDMAN, ibid. (p. 167).
H. D. CARSTANJEN and R. SIZMANN, ibid. (p. 173).
F. H. EISEN and E. UGGERHØJ, ibid. (p. 181).
[29] D. VAN VLIET, Radiat. Eff. **10**, 137 (1971).
[30] G. DELLA MEA, A. V. DRIGO, S. LO RUSSO, P. MAZZOLDI, G. CORNARA, S. YAMAGUCHI, G. G. BENTINI, G. CEMBALI, and F. ZIGNANI, in: Atomic Collisions in Solids, Ed. S. DATZ, B. R. APPLETON, and C. D. MOAK, Plenum Press, New York 1975 (p. 811).

*(Received February 9, 1976)*